Dimerization of visual pigments in vivo

Tao Zhang[a,1], Li-Hui Cao[b,c,1,2], Sandeep Kumar[d,1], Nduka O. Enemchukwu[d,1], Ning Zhang[a,3], Alyssia Lambert[e], Xuchen Zhao[e], Alex Jones[a], Shixian Wang[a], Emily M. Dennis[a], Amrita Fnu[d], Sam Ham[a], Jon Rainier[e], King-Wai Yau[b,c,4], and Yingbin Fu[a,d,4]

[a]Department of Ophthalmology and Visual Sciences, University of Utah, Salt Lake City, UT 84132; [b]Solomon H. Snyder Department of Neuroscience, The Johns Hopkins University School of Medicine, Baltimore, MD 21205; [c]Center for Sensory Biology, The Johns Hopkins University School of Medicine, Baltimore, MD 21205; [d]Department of Ophthalmology, Baylor College of Medicine, Houston, TX 77030; and [e]Department of Chemistry, University of Utah, Salt Lake City, UT 84112

Contributed by King-Wai Yau, June 8, 2016 (sent for review October 9, 2015; reviewed by Jian-xing Ma and Ching-Hwa Sung)

It is a deeply engrained notion that the visual pigment rhodopsin signals light as a monomer, even though many G protein-coupled receptors are now known to exist and function as dimers. Nonetheless, recent studies (albeit all in vitro) have suggested that rhodopsin and its chromophore-free apoprotein, R-opsin, may indeed exist as a homodimer in rod disk membranes. Given the overwhelmingly strong historical context, the crucial remaining question, therefore, is whether pigment dimerization truly exists naturally and what function this dimerization may serve. We addressed this question in vivo with a unique mouse line (*S-opsin*$^{+}$*Lrat*$^{-/-}$) expressing, transgenically, short-wavelength–sensitive cone opsin (S-opsin) in rods and also lacking chromophore to exploit the fact that cone opsins, but not R-opsin, require chromophore for proper folding and trafficking to the photoreceptor's outer segment. In R-opsin's absence, S-opsin in these transgenic rods without chromophore was mislocalized; in R-opsin's presence, however, S-opsin trafficked normally to the rod outer segment and produced functional S-pigment upon subsequent chromophore restoration. Introducing a competing R-opsin transmembrane helix H1 or helix H8 peptide, but not helix H4 or helix H5 peptide, into these transgenic rods caused mislocalization of R-opsin and S-opsin to the perinuclear endoplasmic reticulum. Importantly, a similar peptide-competition effect was observed even in WT rods. Our work provides convincing evidence for visual pigment dimerization in vivo under physiological conditions and for its role in pigment maturation and targeting. Our work raises new questions regarding a potential mechanistic role of dimerization in rhodopsin signaling.

rhodopsin | cone opsin | dimerization | protein trafficking

Rhodopsin and cone pigments mediate scotopic and photopic vision, respectively. They consist of opsin, the apo-protein, and 11-*cis*-retinal, a vitamin A-based chromophore. Light absorption by 11-*cis*-retinal triggers a conformational change in opsin, which in turn initiates a G protein-coupled receptor (GPCR) signaling pathway to lead to vision. Indeed, rhodopsin signaling is a prominent prototypical GPCR pathway from which a huge quantity of mechanistic details about such signaling in general has emerged. All along, it is a dogma that rhodopsin exists and functions as a monomer (1–6). About a decade ago, evidence began to emerge that rhodopsin may exist as a dimer, based on atomic force microscopy and cross-linking experiments performed on rod outer-segment (ROS) disk membranes (7–9). However, this concept remains highly controversial because of the lack of in vivo evidence and also is puzzling because, unlike many GPCRs, monomeric rhodopsin is fully functional with respect to coupling to G protein (2, 4–6, 10) and to interactions with rhodopsin kinase and arrestin (11, 12). In vivo evidence, albeit of paramount importance, is also challenging, because rhodopsin always exists as a single isoform in rod photoreceptors, thus making homomeric, higher-order complexes difficult to distinguish from monomers. We addressed this question by taking advantage of the unique opportunity provided by a mouse line (*S-opsin*$^{+}$*Lrat*$^{-/-}$) that expresses transgenically the short wavelength-sensitive cone opsin (S-opsin) in rods and by exploiting the fact that cone opsins, but not the apoprotein of rhodopsin R-opsin, require chromophore for proper folding and trafficking to the photoreceptor's outer segment (13–17). Our work shows that: (*i*) rhodopsin, and by extension cone pigments, natively mature in vivo in the endoplasmic reticulum (ER) as dimers and traffic as such to the outer segment; (*ii*) in *S-opsin*$^{+}$*Lrat*$^{-/-}$ transgenic rods, R-opsin helps S-opsin fold and traffic by forming heterodimers with it; and (*iii*) the H1 and H8 helices are important for pigment dimerization.

Results

Correct Targeting of S-Opsin to the Outer Segment of *S-opsin*$^{+}$*Rho*$^{+/-}$*Lrat*$^{-/-}$ and *S-opsin*$^{+}$*Rho*$^{+/+}$*Lrat*$^{-/-}$ Rods in the Absence of 11-*cis*-Retinal. We generated various mouse lines by breeding *S-opsin*$^{+}$ with *Rho*$^{-/-}$ and *Lrat*$^{-/-}$ mice (18–20). *Lrat*$^{-/-}$ mice lack lecithin-retinol acyltransferase, which is crucial for the regeneration of 11-*cis*-retinal in the retinal pigment epithelium (21). Previously, we and others found that transgenic cone pigment in rods and transgenic rhodopsin in cones, in an otherwise WT genetic background, signal much like the endogenous pigment in host cells except for a difference in the wavelength of peak absorbance (λ_{max}) (18, 22, 23). In *S-opsin*$^{+}$*Rho*$^{-/-}$*Lrat*$^{-/-}$ rods, which have no endogenous R-opsin and no chromophore, immunolabeling with an S-opsin antibody (18) indicated S-opsin mislocalization to the inner segment, cell body, axon, and synaptic

Significance

Despite in vitro evidence, it remains unclear whether the rod visual pigment rhodopsin exists as dimers in vivo. With a unique mouse line that expresses the blue cone opsin transgenically in rods, we showed that, in the absence of chromophore, the transgenic cone opsin can mature and target to the outer segment if and only if rhodopsin is present to help it along (i.e., forming heterodimers in the endoplasmic reticulum). Furthermore, we have confirmed a key interaction domain for rhodopsin dimerization and show that, again in vivo, rhodopsin maturation and targeting to the outer segment becomes defective when dimerization is disrupted. This work provides in vivo evidence for rhodopsin existing as a dimer.

Author contributions: Y.F. designed research; T.Z., L.-H.C., S.K., N.O.E., N.Z., A.L., X.Z., A.J., S.W., E.M.D., A.F., S.H., and J.R. performed research; T.Z., L.-H.C., S.K., N.O.E., N.Z., K.-W.Y., and Y.F. analyzed data; and K.-W.Y. and Y.F. wrote the paper.

Reviewers: J.-x.M., University of Oklahoma Health Science Center; and C.-H.S., Weill Medical College of Cornell University.

The authors declare no conflict of interest.

[1]T.Z., L.-H.C., S.K., and N.O.E. contributed equally to this work.

[2]Present address: State Key Laboratory of Membrane Biology, Center for Quantitative Biology, McGovern Institute for Brain Research, Peking-Tsinghua Joint Center for Life Science, College of Life Science, Peking University, Beijing, 100871, China.

[3]Present address: Department of Pharmacology, School of Medicine, Case Western Reserve University, Cleveland, OH 44106.

[4]To whom correspondence may be addressed. Email: kyau1@jhmi.edu or yingbin.fu@bcm.edu.

This article contains supporting information online at www.pnas.org/lookup/suppl/doi:10.1073/pnas.1609018113/-/DCSupplemental.

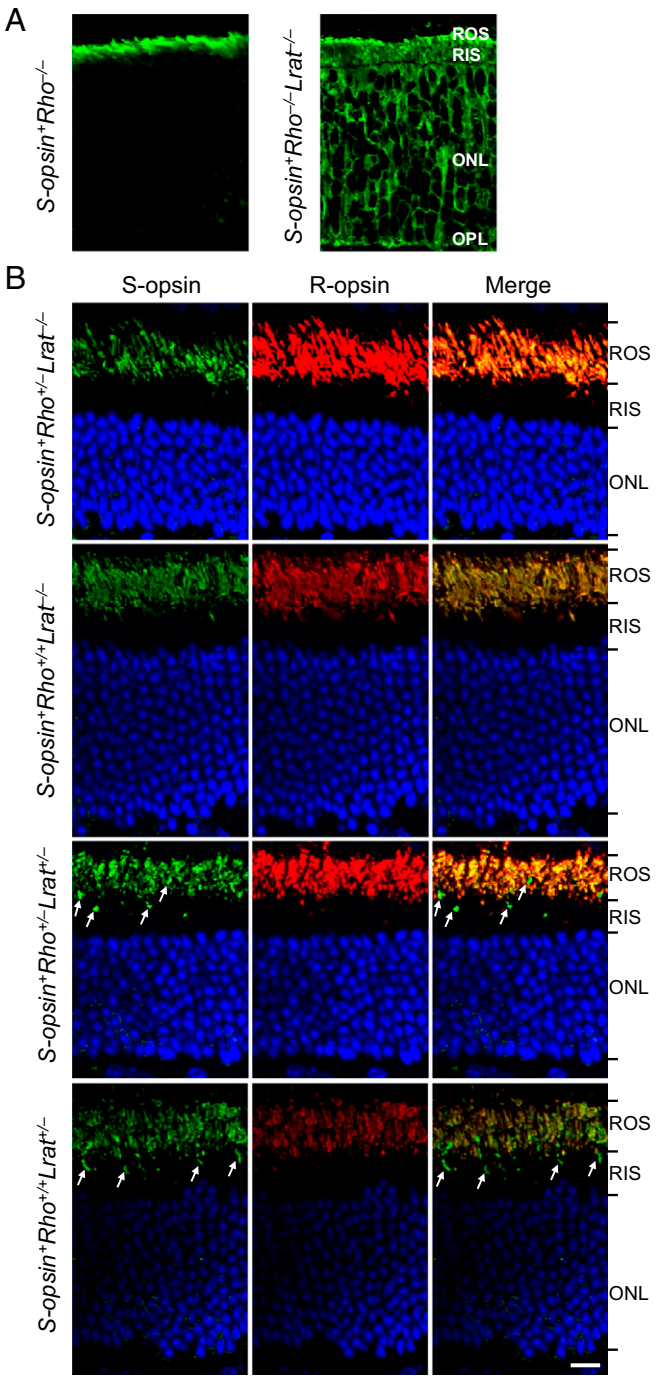

Fig. 1. Trafficking of S-opsin in transgenic mouse rods of different genotypes. (*A*) *S-opsin*$^{+}$*Rho*$^{-/-}$*Lrat*$^{-/-}$ (i.e., lacking chromophore) and its control *S-opsin*$^{+}$*Rho*$^{-/-}$ (i.e., containing chromophore). The age was postnatal day 14 (P14). (*B*) *S-opsin*$^{+}$*Rho*$^{+/-}$*Lrat*$^{-/-}$ and *S-opsin*$^{+}$*Rho*$^{+/+}$*Lrat*$^{-/-}$ (i.e., lacking chromophore) (two *Upper* rows) and their respective controls *S-opsin*$^{+}$*Rho*$^{+/-}$*Lrat*$^{+/-}$ and *S-opsin*$^{+}$*Rho*$^{+/+}$*Lrat*$^{+/-}$ (i.e., containing chromophore) (two *Lower* rows). The age was 2-mo-old. Retinal sections were stained with anti–S-opsin (green) in *A* and *B* and with anti–R-opsin (red) antibodies in *B*. Nuclei were stained with DAPI (blue) in *B*. S-opsin–positive cone photoreceptors (white arrows) are absent in *S-opsin*$^{+}$*Rho*$^{+/-}$*Lrat*$^{-/-}$ and *S-opsin*$^{+}$*Rho*$^{+/+}$*Lrat*$^{-/-}$ retinal sections lacking chromophore because of degeneration but are observable in *S-opsin*$^{+}$*Rho*$^{+/-}$*Lrat*$^{+/-}$ and *S-opsin*$^{+}$*Rho*$^{+/+}$*Lrat*$^{+/-}$ retinal sections containing chromophore. (Scale bar, 10 μm.)

terminus in contrast to the correct rod outer segment (ROS) localization of S-opsin in *S-opsin*$^{+}$*Rho*$^{-/-}$ rods (Fig. 1*A*). In the presence of R-opsin (i.e., in *S-opsin*$^{+}$*Rho*$^{+/-}$*Lrat*$^{-/-}$ or *S-opsin*$^{+}$*Rho*$^{+/+}$*Lrat*$^{-/-}$ rods), however, S-opsin trafficked properly to the ROS despite the absence of chromophore (Fig. 1*B*, *Upper Two Rows*), as it did when chromophore was present (*S-opsin*$^{+}$*Rho*$^{+/-}$*Lrat*$^{+/-}$ and *S-opsin*$^{+}$*Rho*$^{+/+}$*Lrat*$^{+/-}$) (Fig. 1*B*, *Lower Two Rows*; also see the viable cone outer segments indicated by white arrows when chromophore was present), presumably by heteromerizing with R-opsin. S-opsin and R-opsin heteromerization prevents rapid degeneration of *S-opsin*$^{+}$*Rho*$^{-/-}$*Lrat*$^{-/-}$ rods because of ER stress caused by misfolded and mistrafficked S-opsin [see Fig. S1 comparing the ROS, rod inner segments (RIS) and outer nuclear layer (ONL) in *S-opsin*$^{+}$*Rho*$^{-/-}$*Lrat*$^{-/-}$ and *S-opsin*$^{+}$*Rho*$^{+/-}$*Lrat*$^{-/-}$ mice at age 1 mo] (16). In the above experiments, we used *S-opsin*$^{+}$*Rho*$^{+/-}$*Lrat*$^{-/-}$ and *S-opsin*$^{+}$*Rho*$^{+/+}$*Lrat*$^{-/-}$ mice older than 1 mo in which most of the S-opsin–expressing cones had already died from the lack of chromophore, thus minimizing confounding signals from those cones (13, 15, 16). As a negative control for a generalized disruption of protein targeting to the ROS in the absence of chromophore and R-opsin, we also examined the localization of a rod cyclic nucleotide-gated cation channel subunit, CNGA1, a membrane protein mediating phototransduction in ROS. Even without R-opsin, and in either the absence (*S-opsin*$^{+}$*Rho*$^{-/-}$*Lrat*$^{-/-}$) or presence (*S-opsin*$^{+}$*Rho*$^{-/-}$*Lrat*$^{+/-}$) of chromophore, CNGA1 was targeted properly to the ROS (Fig. S2).

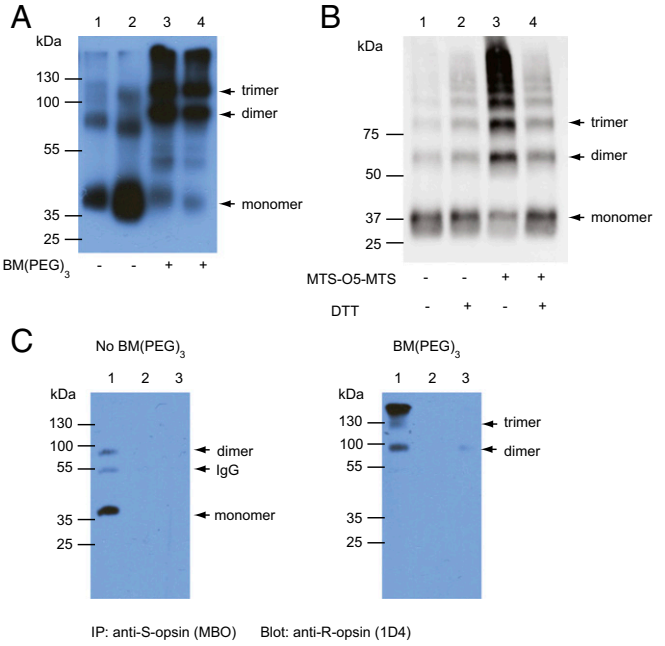

Fig. 2. Chemical cross-linking of cone and rod opsins in ROS membranes of different mouse lines followed by Western blot analysis. (*A*) Non–cross-linked (lanes 1 and 2) and cross-linked (lanes 3 and 4) S-opsin from ROS membranes of *S-opsin*$^{+}$*Rho*$^{+/-}$*Lrat*$^{-/-}$ mice (lanes 1 and 3) and *S-opsin*$^{+}$*Rho*$^{-/-}$*Lrat*$^{+/-}$ mice (lanes 2 and 4) following treatment with a noncleavable reagent, $BM(PEG)_3$. The loading variability in different lanes was caused by the variable yield of the isolated ROS membrane fraction because the procedure was carried out in darkness. (*B*) Cross-linking of S-opsin in ROS membranes of *S-opsin*$^{+}$*Rho*$^{+/-}$*Lrat*$^{-/-}$ mice with a cleavable reagent, MTS-O5-MTS. Samples were analyzed in the absence (lanes 1 and 2) and presence (lanes 3 and 4) of cross-linker. The even-numbered lanes were treated with DTT before the gel was run. Arrows indicate the locations of monomers, dimers, and trimers. (*C*) Coimmunoprecipitation to detect dimeric interaction between S-opsin and R-opsin. Non–cross-linked and cross-linked ROS membranes from *S-opsin*$^{+}$*Rho*$^{+/-}$*Lrat*$^{-/-}$ (lane1), *S-opsin*$^{+}$*Rho*$^{-/-}$*Lrat*$^{+/-}$ (lane 2), and *Rho*$^{+/-}$*Lrat*$^{-/-}$ (lane 3) mice were immunoprecipitated with an anti–S-opsin antibody, MBO, and were analyzed by immunoblotting with an anti–R-opsin antibody, 1D4. A very faint band in the cross-linked sample (*Right*, lane 3) is likely caused by some nonspecific interaction between the abundant R-opsin and protein A/G beads.

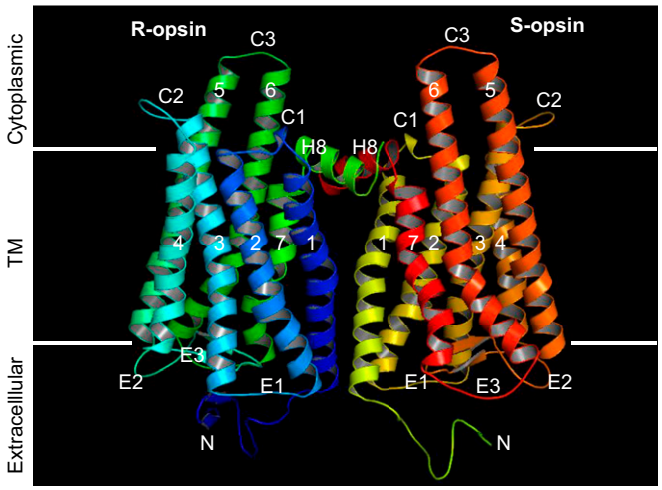

Fig. 3. Structure of an R–S heterodimer via H1/H8 interface. The R–S heterodimer was modeled according to the crystal structure of the ligand-free opsin homodimer (PDB ID code 3CAP) (41) by homology modeling. The two monomers in the asymmetric unit are viewed from within the membrane. Seven transmembrane helices (1–7), extracellular loops (E1–E3), cytoplasmic loops (C1–C3), and a cytoplasmic helix (H8) are indicated. The figure was created with PyMOL (www.pymol.org/).

Dimerization of S-Opsin with R-Opsin in *S-opsin*$^{+}$*Rho*$^{+/-}$*Lrat*$^{-/-}$ Rods. To probe for R/S-opsin heteromerization in transgenic rods, we performed cross-linking experiments on ROS membranes isolated from dark-adapted *S-opsin*$^{+}$*Rho*$^{+/-}$*Lrat*$^{-/-}$ mice using a noncleavable homobifunctional bis-maleimide reagent, BM(PEG)$_3$ (24), followed by Western blot analysis with an anti–S-opsin (18) antibody. Without cross-linking, S-opsin was detected mainly as monomers in denaturing SDS/PAGE (Fig. 2*A*, lane 1). With cross-linking, we found S-opsin predominantly as dimers and oligomers, presumably mostly with R-opsin (Fig. 2*A*, lane 3). The reagent also cross-linked S-pigment in *S-opsin*$^{+}$*Rho*$^{-/-}$*Lrat*$^{+/-}$ rods (i.e., with chromophore but no R-opsin), in this case giving S-pigment homomers (Fig. 2*A*, lane 4). To confirm the specificity of cross-linking, we did cross-linking experiment using a cleavable methanethiosulfonate (MTS) cross-linker, MTS-O5-MTS (24). MTS-O5-MTS treatment shifted S-opsin from mainly monomers to dimers and oligomers (Fig. 2*B*, lane 3). DTT treatment, which cleaved the disulfide bond formed by MTS-O5-MTS, converted the higher-molecular-weight bands back to primarily monomers (Fig. 2*B*, lane 4), similar to samples without MTS-O5-MTS (Fig. 2*B*, lanes 1 and 2). This experiment suggests that the high-molecular-weight bands in the MTS-O5-MTS–treated samples were the result of cross-linking reactions and not nonspecific oligomerization. To confirm that the dimers in *S-opsin*$^{+}$*Rho*$^{+/-}$*Lrat*$^{-/-}$ ROS were indeed R/S-opsin heteromers, we performed immunoprecipitation on ROS membrane homogenate from these mice with the mouse blue opsin (MBO) antibody (18) followed by Western blot analysis with an anti–R-opsin antibody, 1D4 (25). Indeed, the anti–S-opsin antibody coimmunoprecipitated S-opsin and R-opsin in both non–cross-linked (Fig. 2*C*, *Left*, lane 1) and cross-linked ROS membrane fractions (Fig. 2*C*, *Right*, lane 1). The major bands were R-opsin monomers in the non–cross-linked samples but were R/S-opsin heterodimers and heterooligomers in the cross-linked samples, as is consistent with the results shown in Fig. 2*A*. As controls, no R-opsin was coimmunoprecipitated with S-opsin in the *S-opsin*$^{+}$*Rho*$^{-/-}$*Lrat*$^{+/-}$ sample (because R-opsin was absent) (Fig. 2*C*, lane 2 in both panels) or in the *Rho*$^{+/-}$*Lrat*$^{-/-}$ sample (because S-opsin was absent) (Fig. 2*C*, lane 3 in both panels). Thus, S-opsin indeed heteromerized with R-opsin in *S-opsin*$^{+}$*Rho*$^{+/-}$*Lrat*$^{-/-}$ rods, underlying the former's trafficking shown in Fig. 1. This property in turn suggests that R- and S-opsins must have sufficiently similar 3D topologies to allow R/S-opsin interactions (i.e., homologous to R/R-opsin interactions) and similar amino acid sequences for cross-linking. For example, both opsins have a key cysteine in H8 [C316 in R-opsin (24) and C311 in S-opsin] close enough to each other in a tail-to-tail dimer conformation for cross-linking by BM(PEG)$_3$ and MTS-O5-MTS (Fig. 3 and Fig. S3). On the other hand, the presence of oligomers

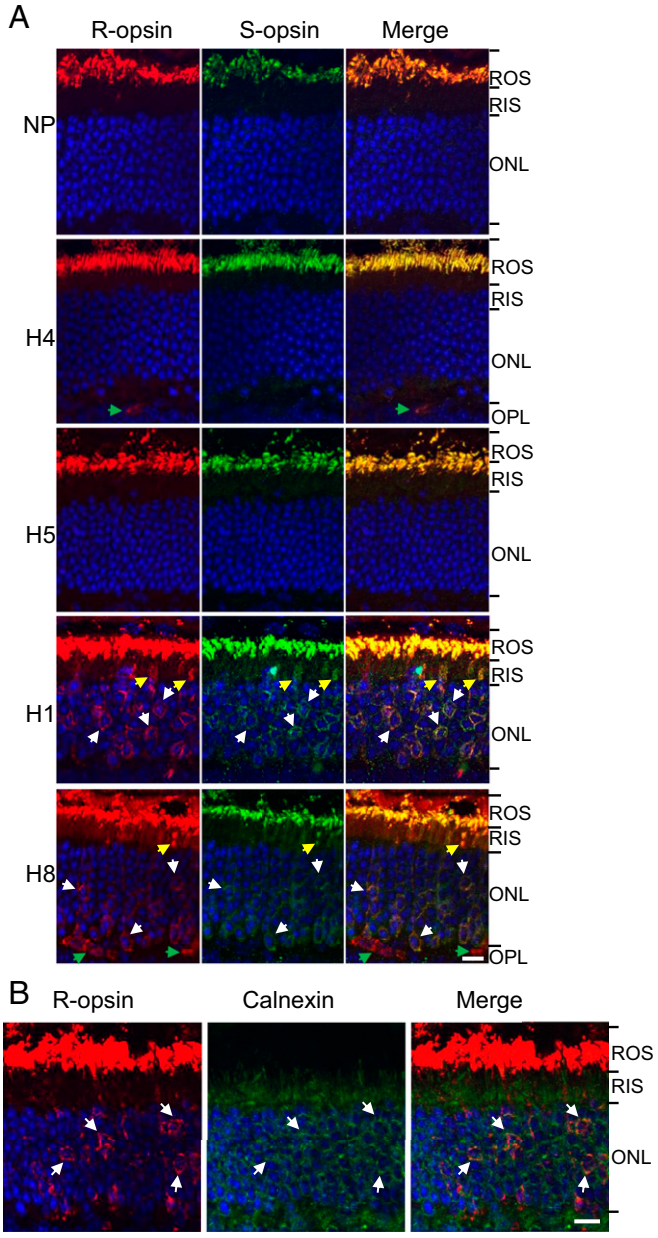

Fig. 4. Peptide-competition experiments in *S-opsin*$^{+}$*Rho*$^{+/-}$*Lrat*$^{-/-}$ rods. (*A*) Subretinal injection of NP-encapsulated R-opsin H1 and 8 peptides, but not R-opsin H4 and H5 peptides, caused mislocalization of both R-opsin and S-opsin in *S-opsin*$^{+}$*Rho*$^{+/-}$*Lrat*$^{-/-}$ rods. Mouse retinas were stained with anti–R-opsin (red) and anti–S-opsin (green) antibodies. White arrows indicate mislocalized R-opsin and S-opsin in the perinuclear region. Yellow arrows indicate mislocalized R-opsin and S-opsin in the inner segment. Green arrows indicate retinal blood vessels in the outer plexiform layer (OPL) labeled by the Cy3-conjugated goat anti-mouse secondary antibody. (*B*) Mislocalized R-opsin caused by subretinal injection of R-opsin H8 peptide colocalizes with the ER marker Calnexin in *S-opsin*$^{+}$*Rho*$^{+/-}$*Lrat*$^{-/-}$ rods. *S-opsin*$^{+}$*Rho*$^{+/-}$*Lrat*$^{-/-}$ mice were injected with NP-encapsulated R-opsin H8 peptide. Mouse retinas were stained with R-opsin (red) and Calnexin (green) antibodies. Nuclei were stained with DAPI (blue). White arrows indicate the colocalization of mislocalized R-opsin with Calnexin in the perinuclear region. (Scale bars, 10 μm.)

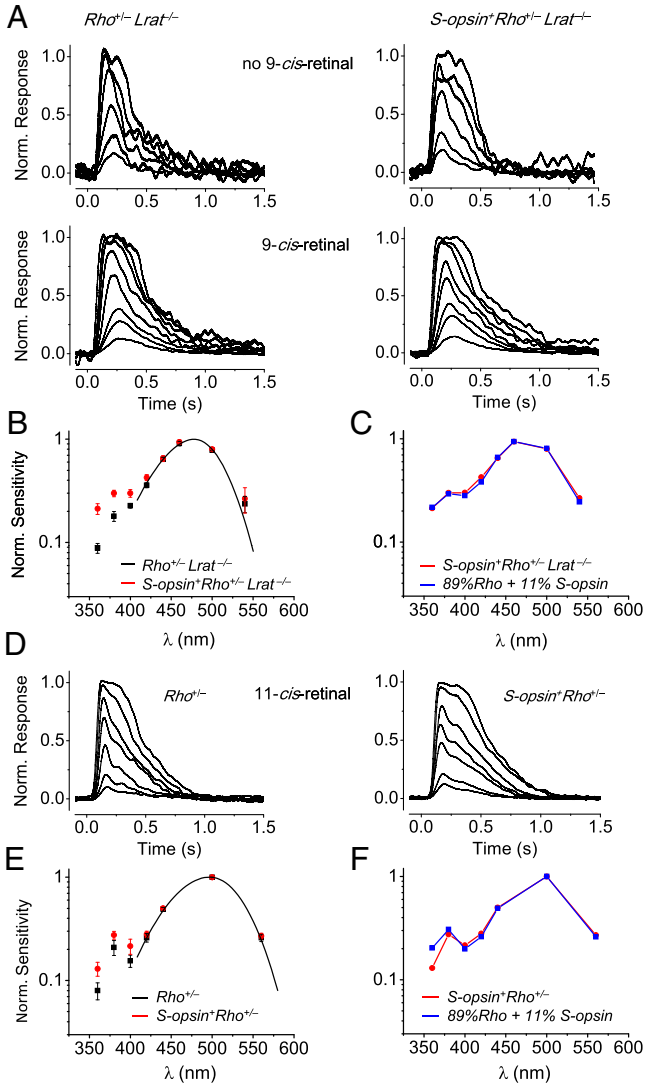

Fig. 5. Flash responses and action spectra of $Rho^{+/-}Lrat^{-/-}$ and $S\text{-}opsin^{+}Rho^{+/-}Lrat^{-/-}$ rods after perfusion with 9-*cis*-retinal (*A*–*C*), compared with those of $Rho^{+/-}$ and $S\text{-}opsin^{+}Rho^{+/-}$ rods after perfusion with 11-*cis*-retinal (*D*–*F*). (*A*) Flash families from $Rho^{+/-}Lrat^{-/-}$ and $S\text{-}opsin^{+}Rho^{+/-}Lrat^{-/-}$ rods before and after 9-*cis*-retinal treatment (four separate cells). A 12.1-ms flash at time 0 delivered 1,153, 2,772, 8,560, 15,400, 25,152, and 77,576 photons·μm^{-2} at 480 nm before 9-*cis*-retinal treatment and delivered 15.6, 35.7, 60.3, 105.4, 183.5, 250, 534, and 920 photons·μm^{-2} at 480 nm after 9-*cis*-retinal treatment. The saturated response amplitude was very small for rods of both lines before chromophore treatment (typically <2 pA) but increased substantially after treatment. (See Table S1 for collected data.) The flash sensitivity of both lines was also ∼60-fold higher after 9-*cis*-retinal treatment than before treatment, and the response integration time, t_{int}, increased from ∼220 ms to 370 ms for the two cells. (*B*) The action spectra show $S\text{-}opsin^{+}Rho^{+/-}Lrat^{-/-}$ rods are more sensitive to UV than $Rho^{+/-}Lrat^{-/-}$ rods. Shown are averaged, normalized data from 11 $Rho^{+/-}Lrat^{-/-}$ rods and 13 $S\text{-}opsin^{+}Rho^{+/-}Lrat^{-/-}$ rods. The black curve is the spectral template for isorhodopsin with λ_{max} at 477 nm. Incidentally, the rise in sensitivity of R pigment at λ_{max} <400 nm does not belong to the main (α-) band of the pigment's absorption spectrum and is not included in the fit by template (see also ref. 18), although it is included in the overall calculations in *C*. (*C*) The action spectrum of $S\text{-}opsin^{+}Rho^{+/-}Lrat^{-/-}$ rods (red points) was fit by a linear combination of isorhodopsin data in *B* (black points) and a spectral template for 9-*cis*-S-pigment with λ_{max} at 365 nm, giving a ratio of 89:11% (blue). (*D*) Flash families from $Rho^{+/-}$ and $S\text{-}opsin^{+}Rho^{+/-}$ rods after 11-*cis*-retinal treatment. Although both rods had 11-*cis*-retinal throughout life, we nonetheless pretreated them with 11-*cis*-retinal to remove any bare opsin (42), providing a better comparison with the data presented in *A*–*C* above. A 12.1-ms flash at time 0 delivered 4.5, 7.8, 16.7, 35.7, 60.2, 115, 204, and 472 photons·μm^{-2} at 500 nm in both cases. (*E*) The action spectrum of $S\text{-}opsin^{+}Rho^{+/-}$ rods showed an increase in UV sensitivity compared with that of $Rho^{+/-}$ rods. Shown are averaged, normalized data from 6 $Rho^{+/-}$ rods and 12 $S\text{-}opsin^{+}Rho^{+/-}$ rods. The black curve is spectral template for 11-*cis*-rhodopsin with λ_{max} at 498 nm. Details are as in *B*. (*F*) The action spectrum of $S\text{-}opsin^{+}Rho^{+/-}$ rods (red points) was fit by a linear combination of 11-*cis*-rhodopsin's data in *E* (black points) and a spectral template for 11-*cis*-S-pigment with λ_{max} at 360 nm, giving a ratio of 89:11% (blue). Error bars in *B* and *E* indicate SEM. See *SI Methods* for the procedure of spectral fitting.

in the cross-linking experiments also may suggest higher-order complexes involving other cysteine pairs between the pigment proteins captured by the cross-linker (see ref. 24 and below).

Disruption by Helix Peptides of R- and S-Opsin Trafficking in $S\text{-}opsin^{+}Rho^{+/-}Lrat^{-/-}$ Rods. Two dimer interfaces between rhodopsin protomers have been suggested, with the first being formed by transmembrane helices 4 and 5 (i.e., H4/H5–H4/H5) (8, 9) and the second formed by transmembrane helix 1 and cytoplasmic helix 8 (i.e., H1/H8–H1/H8) (24). To determine whether the two interfaces were involved in the R/S-opsin interaction that we observed in vivo, we used peptides derived from these R-opsin domains to see whether they would disrupt, by competition (26–28), the R/S-opsin interaction and therefore trafficking. Each peptide was encapsulated in biodegradable polylactic acid-polyethylene oxide (PLA-PEO) nanoparticles (NPs) (29) for sustained delivery and was injected subretinally into $S\text{-}opsin^{+}Rho^{+/-}Lrat^{-/-}$ mouse eyes. Retinal sections were analyzed 6 d after injection. Both the H1 and H8 peptides caused mislocalization of R-opsin to the inner segment (yellow arrows in Fig. 4*A*) and the perinuclear ER region in the ONL (white arrows in Fig. 4*A* and white arrows indicating R-opsin colocalization with the ER marker Calnexin in Fig. 4*B*). S-opsin mislocalization was observed also (Fig. 4*A*). Injection of the carrier NPs alone (Fig. 4*A*) or of NPs encapsulating the rhodopsin H4 or H5 peptides (Fig. 4*A*) did not interfere with R-opsin and S-opsin trafficking.

Functional S-Opsin After Trafficking to $S\text{-}opsin^{+}Rho^{+/-}Lrat^{-/-}$ ROS. To explore whether the S-opsin helped by R-opsin to traffic to the ROS in the $S\text{-}opsin^{+}Rho^{+/-}Lrat^{-/-}$ retina was indeed functional, we perfused the isolated retina of this genotype in darkness with 9-*cis*-retinal [this chromophore was found to be naturally present in trace amounts in $Lrat^{-/-}$ retina (13), although far from sufficient for normal S-opsin trafficking (13, 19)] and made recordings from single rods with suction-pipette recording. The photosensitivity of both $Rho^{+/-}Lrat^{-/-}$ and $S\text{-}opsin^{+}Rho^{+/-}Lrat^{-/-}$ rods after chromophore treatment increased by as much as ∼60-fold (Fig. 5*A* and legend), reflecting the regeneration of R-opsin into isorhodopsin (i.e., rhodopsin containing 9-*cis*-retinal). The dim flash–response kinetics also became slower after treatment (see legend of Fig. 5*A* and collected data in Table S1) because of the removal of the bleaching adaptation associated with chromophore-free R-opsin. Importantly, a comparison in the action spectra of 9-*cis*-retinal–treated $Rho^{+/-}Lrat^{-/-}$ rods and $S\text{-}opsin^{+}Rho^{+/-}Lrat^{-/-}$ rods showed that the latter had extra photosensitivity in the UV region (red points in Fig. 5*B*), reflecting functional S-pigment (λ_{max} = 365 nm with 9-*cis*-retinal). Fitting the action spectrum of $S\text{-}opsin^{+}Rho^{+/-}Lrat^{-/-}$ rods with a linear combination of the isorhodopsin data (black points in Fig. 5*B*) and the spectral template of 9-*cis*-S-cones, we arrived at an isorhodopsin/S-cone pigment ratio in the ROS of 89/11% (Fig. 5*C*). We made similar measurements on $Rho^{+/-}$ and $S\text{-}opsin^{+}Rho^{+/-}$ rods, which have a normal 11-*cis*-retinal supply throughout life and therefore never have trafficking problems with their S-pigment, and arrived at a similar rhodopsin/S-pigment ratio in the ROS of 89/11% (Fig. 5 *D*–*F* and Table S1) (also see ref. 18). Thus, virtually all S-opsin in $S\text{-}opsin^{+}Rho^{+/-}Lrat^{-/-}$ rods trafficked successfully to the ROS through heteromerization with R-opsin; this result is not unreasonable, given the large excess of R-opsin available to S-opsin.

Disruption by Helix Peptides of Rhodopsin Trafficking in WT Rods. We tested whether subretinal delivery of NP-encapsulated H1 or H8 peptide could disrupt even the normal trafficking of rhodopsin in WT (i.e., *Lrat*$^{+/+}$) rods. Neither peptide had an effect (Fig. S4). Possibly, homomeric R–R interaction is stronger than heteromeric R–S interaction and resists competition by the peptide. Accordingly, we tried to overcome this putative resistance by adding an ER-targeting signal, KDEL, at the C terminus of the competing peptide to increase its effective concentration in the ER. Indeed, in cell culture, the H8-KDEL peptide exhibited virtually complete colocalization with an ER marker (white arrowheads in Fig. 6*A*, *Lower Right*), whereas the H8 peptide only partially colocalized with the ER marker (white arrows indicating nonoverlapped peptide signals in Fig. 6*A*, *Upper Right*). The increased ER targeting efficiency of H8-KDEL is likely through the retrograde transport system from Golgi to ER via the KDEL receptors (30–32). In vivo, the H8-KDEL peptide caused mislocalization of rhodopsin to the inner segment and perinuclear ER region (yellow and white arrows, respectively, in Fig. 6*B*, *Bottom Left*), with the latter indicated by Calnexin labeling (Fig. 6*B*, *Bottom Center*). The same treatment with NP alone or with the H4-KDEL peptide had no effect (Fig. 6*B*, *Top* and *Middle Rows*). Thus, the H1/H8 domains rather than the H4/H5 domains may be the primary protomer–protomer interface in R/R-opsin and R/S-opsin dimerization during biosynthesis and targeting, although secondary interactions in the H4/H5 domains and even others are still possible in the ROS (33–36). This result is consistent with the cross-linking experiment involving BM(PEG)$_3$ and MTS-O5-MTS, whose extended S–S distance of 2.1 and 2.6 nm, respectively, is within the predicted C316–C316 distance of 2.1–2.9 nm in the rhodopsin H1/H8 dimer (2.4 nm in the R/S-opsin heterodimer) (Fig. S3) (24).

Discussion

By exploiting transgenic *S-opsin*$^{+}$*Rho*$^{+/-}$*Lrat*$^{-/-}$ and *S-opsin*$^{+}$*Rho*$^{+/+}$*Lrat*$^{-/-}$ rods, we have demonstrated that R-opsin is able to facilitate the folding and proper trafficking of coexpressed S-opsin when the latter fails to do so by itself in the absence of chromophore. We conclude that heteromerization between R-opsin and S-opsin exists in the transgenic rod, a conclusion also supported by cross-linking, coimmunoprecipitation, and peptide-competition experiments. These experiments together provide in vivo evidence for visual pigment dimerization that begins during its biosynthesis at the ER. Importantly, we found the same specific competing-peptide effect on rhodopsin maturation and targeting in WT rods, thus extending the conclusion to the completely native and physiological situation. Two possibilities might account for H8-mediated rhodopsin mislocalization. One is that dimerization is required for rhodopsin trafficking. Thus, disruption of rhodopsin dimerization leads to trafficking defects. Alternatively, rhodopsin folding and dimerization are coupled during protein synthesis, as suggested by the rescue of the S-opsin folding defect in *S-opsin*$^{+}$*Rho*$^{+/-}$*Lrat*$^{-/-}$ mice. Disruption of rhodopsin dimerization may cause folding defects and subsequently affect trafficking. In both cases, our data suggest that dimerization involving homotypic H1 and H8 interactions is critical for correct visual pigment folding, maturation, and targeting. Recently, an in vitro study based on peptide competition suggests the involvement of two interfaces (i.e., H1/H2 and H4/H5) between the two rhodopsin protomers in the dimer (36). That work differs from our in vivo study in that it addresses the state of rhodopsin after the protein has reached the ROS, whereas our work addresses rhodopsin dimer formation in the ER. It is possible that rhodopsin first forms dimers in the ER via the H1/H8 interface (Fig. 3), followed by higher-order oligomerization involving multiple interfaces after reaching the ROS (perhaps promoted by the very high concentration of rhodopsin). Indeed, the possible existence of higher-order visual pigment oligomerization in the ROS has been suggested by experiments involving cross-linkers (this work and refs. 24 and 37) and cryoelectron tomography (38). Separately, visual pigment dimerization has interesting implications for mouse cones because they coexpress M and S pigments in the same cell, with an

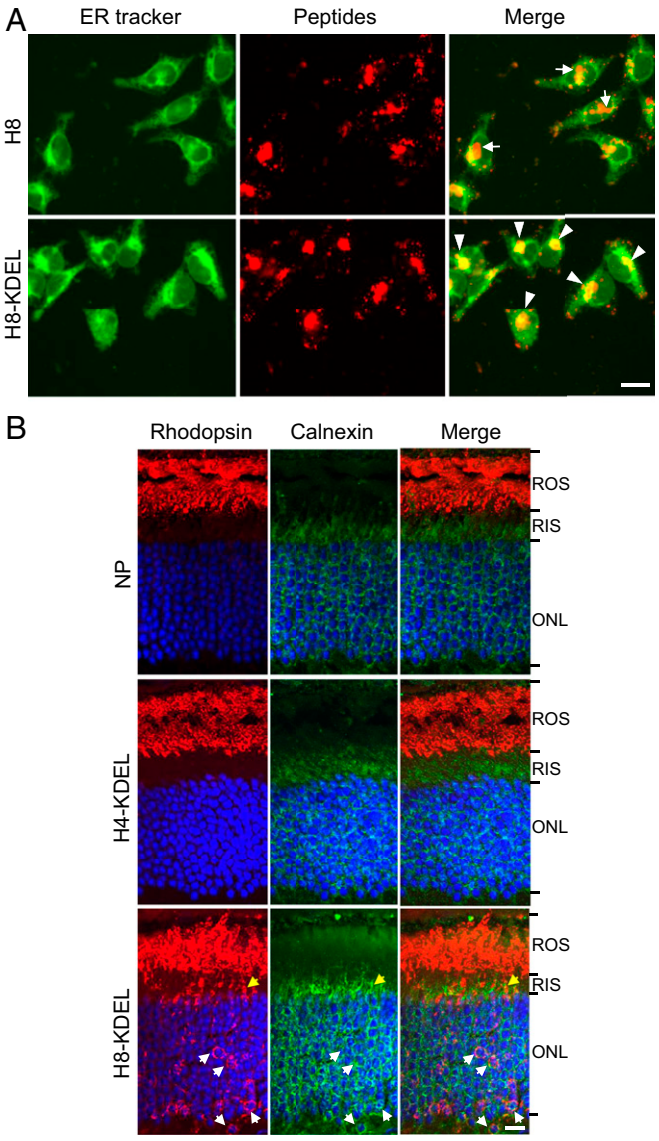

Fig. 6. Peptide-competition experiments in WT rods. (*A*) Rhodamine-labeled H8-KDEL or H8 peptides (red) were delivered to HEK293 cells followed by live-cell imaging. The ER was labeled with ER-Tracker Green. White arrows indicate H8 peptides outside the ER. White arrowheads indicate the complete colocalization of H8-KDEL with ER-Tracker. (*B*) Subretinal injection of NP-encapsulated R-opsin H8-KDEL peptide but not R-opsin H4-KDEL peptide caused mislocalization of rhodopsin in WT rods. Mouse retinas were stained with anti–R-opsin (red) and anti-Calnexin (green) antibodies. White arrows indicate mislocalized R-opsin in the perinuclear ER region, which is colocalized with the ER marker Calnexin. Yellow arrows indicate mislocalized R-opsin in the inner segment. (Scale bars, 20 μm in *A* and 10 μm in *B*.)

M/S pigment ratio dependent on cell location in the retina (39); thus, conceivably, M and S pigment homodimers as well as M/S pigment heterodimers may coexist in a given mouse cone. The important remaining question is whether a pigment dimer is stable during its lifetime or if mature dimers and monomers exist in equilibrium in the outer segment. If dimers are indeed stable, then it is possible that, besides being important for rhodopsin maturation and targeting, the dimer configuration may actually have a subtle, hitherto unknown mechanistic role in rhodopsin's activation of transducin and possibly even its interactions with rhodopsin kinase and arrestin. These are new questions to ponder, even though rhodopsin monomers themselves are capable of these functions (2, 4–6, 10–12). Last, more than 100 mutations of rhodopsin are associated

with the degenerative disease autosomal-dominant retinitis pigmentosa (ADRP), with WT and mutant rhodopsin being copresent in rods. Some of the pathology conceivably could involve defective dimerization of rhodopsin in the ER. Understanding this process might help in the development of future therapies for this class of ADRP.

Methods

Lrat$^{-/-}$, *S-opsin*$^{+}$, and *Rho*$^{-/-}$ mice were generated previously (18–20). All animal experiments were approved by the Institutional Animal Care and Use Committees at Baylor College of Medicine, the University of Utah, and the Johns Hopkins University School of Medicine and were performed in accordance with the Association for Research in Vision and Ophthalmology Statement for the Use of Animal in Ophthalmic and Vision Research. Peptides corresponding to H1 (WQFSMLAAYMFLLIVLGFPINFLTLYVTV), H4 (HAIMGVVFTWIMALACAAPPLV), H5 (ESFVIYMFVVHFTIPMIVIFFCYGQLV), H8 (NKQFRNCMLTTL), H4-KDEL (HAIMGVVFTWIMALACAAPPLVKDEL), and H8-KDEL (NKQFRNCMLTTLKDEL) of mouse rhodopsin were synthesized and purified by Selleck Chemicals LLC. Rhodamine-labeled H8 or H8-KDEL via the N terminus was synthesized and purified by Peptide 2.0 Inc. NPs were fabricated as previously described (29). KDEL is a C-terminal signal for the localization in the ER of many soluble proteins residing in the ER lumen in eukaryotic cells (40). Chemical cross-linking was performed under dim red light as previously described (24). Immunohistochemistry, immunoprecipitation, Western blot, subretinal injection, and electrical recording were done with standard protocols. Detailed methods are described in *SI Methods*.

ACKNOWLEDGMENTS. We thank Jeannie Chen for the *S-opsin*$^{+}$ mouse line and the S-opsin antibody; Wolfgang Baehr for the *Lrat*$^{-/-}$ mouse line; Janis Lem for the *Rho*$^{-/-}$ mouse line; Robert S. Molday for the 1D4 and 1D1 antibodies; Thomas Huber for providing information on cross-linkers; and Zheng Jiang, Xiaozhi Ren, Yanghui Sheng, Wendy W.-S. Yue, Katie Pennington, and Jacki Roberts for comments on the manuscript. T.Z. was supported by a Career Initiation Research Grant Award from Knights Templar; Y.F. was supported by NIH Grant EY022614, the E. Matilda Ziegler Foundation for the Blind, a Career Development Award from Research to Prevent Blindness (RPB), NIH Core Grant 2P30EY002520, and an unrestricted RPB grant to the Department of Ophthalmology at Baylor College of Medicine; and K.-W.Y. was supported by NIH Grant EY06837 and the António Champalimaud Vision Award from the Champalimaud Foundation.

1. Chabre M, le Maire M (2005) Monomeric G-protein-coupled receptor as a functional unit. *Biochemistry* 44(27):9395–9403.
2. Ernst OP, Gramse V, Kolbe M, Hofmann KP, Heck M (2007) Monomeric G protein-coupled receptor rhodopsin in solution activates its G protein transducin at the diffusion limit. *Proc Natl Acad Sci USA* 104(26):10859–10864.
3. Chabre M, Cone R, Saibil H (2003) Biophysics: Is rhodopsin dimeric in native retinal rods? *Nature* 426(6962):30–31, discussion 31.
4. Whorton MR, et al. (2007) A monomeric G protein-coupled receptor isolated in a high-density lipoprotein particle efficiently activates its G protein. *Proc Natl Acad Sci USA* 104(18):7682–7687.
5. Whorton MR, et al. (2008) Efficient coupling of transducin to monomeric rhodopsin in a phospholipid bilayer. *J Biol Chem* 283(7):4387–4394.
6. Banerjee S, Huber T, Sakmar TP (2008) Rapid incorporation of functional rhodopsin into nanoscale apolipoprotein bound bilayer (NABB) particles. *J Mol Biol* 377(4):1067–1081.
7. Fotiadis D, et al. (2004) The G protein-coupled receptor rhodopsin in the native membrane. *FEBS Lett* 564(3):281–288.
8. Fotiadis D, et al. (2003) Atomic-force microscopy: Rhodopsin dimers in native disc membranes. *Nature* 421(6919):127–128.
9. Liang Y, et al. (2003) Organization of the G protein-coupled receptors rhodopsin and opsin in native membranes. *J Biol Chem* 278(24):21655–21662.
10. Bayburt TH, Leitz AJ, Xie G, Oprian DD, Sligar SG (2007) Transducin activation by nanoscale lipid bilayers containing one and two rhodopsins. *J Biol Chem* 282(20):14875–14881.
11. Bayburt TH, et al. (2011) Monomeric rhodopsin is sufficient for normal rhodopsin kinase (GRK1) phosphorylation and arrestin-1 binding. *J Biol Chem* 286(2):1420–1428.
12. Tsukamoto H, Sinha A, DeWitt M, Farrens DL (2010) Monomeric rhodopsin is the minimal functional unit required for arrestin binding. *J Mol Biol* 399(3):501–511.
13. Fan J, Rohrer B, Frederick JM, Baehr W, Crouch RK (2008) Rpe65-/- and Lrat-/- mice: Comparable models of leber congenital amaurosis. *Invest Ophthalmol Vis Sci* 49(6):2384–2389.
14. Znoiko SL, et al. (2005) Downregulation of cone-specific gene expression and degeneration of cone photoreceptors in the Rpe65-/- mouse at early ages. *Invest Ophthalmol Vis Sci* 46(4):1473–1479.
15. Zhang H, et al. (2008) Trafficking of membrane-associated proteins to cone photoreceptor outer segments requires the chromophore 11-cis-retinal. *J Neurosci* 28(15):4008–4014.
16. Zhang T, Zhang N, Baehr W, Fu Y (2011) Cone opsin determines the time course of cone photoreceptor degeneration in Leber congenital amaurosis. *Proc Natl Acad Sci USA* 108(21):8879–8884.
17. Insinna C, et al. (2012) An S-opsin knock-in mouse (F81Y) reveals a role for the native ligand 11-cis-retinal in cone opsin biosynthesis. *J Neurosci* 32(23):8094–8104.
18. Shi G, Yau KW, Chen J, Kefalov VJ (2007) Signaling properties of a short-wave cone visual pigment and its role in phototransduction. *J Neurosci* 27(38):10084–10093.
19. Batten ML, et al. (2004) Lecithin-retinol acyltransferase is essential for accumulation of all-trans-retinyl esters in the eye and in the liver. *J Biol Chem* 279(11):10422–10432.
20. Lem J, et al. (1999) Morphological, physiological, and biochemical changes in rhodopsin knockout mice. *Proc Natl Acad Sci USA* 96(2):736–741.
21. Ruiz A, et al. (1999) Molecular and biochemical characterization of lecithin retinol acyltransferase. *J Biol Chem* 274(6):3834–3841.
22. Kefalov V, Fu Y, Marsh-Armstrong N, Yau KW (2003) Role of visual pigment properties in rod and cone phototransduction. *Nature* 425(6957):526–531.
23. Fu Y, Kefalov V, Luo DG, Xue T, Yau KW (2008) Quantal noise from human red cone pigment. *Nat Neurosci* 11(5):565–571.
24. Knepp AM, Periole X, Marrink SJ, Sakmar TP, Huber T (2012) Rhodopsin forms a dimer with cytoplasmic helix 8 contacts in native membranes. *Biochemistry* 51(9):1819–1821.
25. MacKenzie D, Arendt A, Hargrave P, McDowell JH, Molday RS (1984) Localization of binding sites for carboxyl terminal specific anti-rhodopsin monoclonal antibodies using synthetic peptides. *Biochemistry* 23(26):6544–6549.
26. Harikumar KG, et al. (2012) Glucagon-like peptide-1 receptor dimerization differentially regulates agonist signaling but does not affect small molecule allostery. *Proc Natl Acad Sci USA* 109(45):18607–18612.
27. Wang J, He L, Combs CA, Roderiquez G, Norcross MA (2006) Dimerization of CXCR4 in living malignant cells: Control of cell migration by a synthetic peptide that reduces homologous CXCR4 interactions. *Mol Cancer Ther* 5(10):2474–2483.
28. Harikumar KG, et al. (2006) Transmembrane segment peptides can disrupt cholecystokinin receptor oligomerization without affecting receptor function. *Biochemistry* 45(49):14706–14716.
29. Kim H, Csaky KG (2010) Nanoparticle-integrin antagonist C16Y peptide treatment of choroidal neovascularization in rats. *J Control Release* 142(2):286–293.
30. Sandvig K, van Deurs B (2002) Transport of protein toxins into cells: Pathways used by ricin, cholera toxin and Shiga toxin. *FEBS Lett* 529(1):49–53.
31. Miesenböck G, Rothman JE (1995) The capacity to retrieve escaped ER proteins extends to the trans-most cisterna of the Golgi stack. *J Cell Biol* 129(2):309–319.
32. Raykhel I, et al. (2007) A molecular specificity code for the three mammalian KDEL receptors. *J Cell Biol* 179(6):1193–1204.
33. Edwards PC, et al. (2004) Crystals of native and modified bovine rhodopsins and their heavy atom derivatives. *J Mol Biol* 343(5):1439–1450.
34. Salom D, et al. (2006) Crystal structure of a photoactivated deprotonated intermediate of rhodopsin. *Proc Natl Acad Sci USA* 103(44):16123–16128.
35. Periole X, Huber T, Marrink SJ, Sakmar TP (2007) G protein-coupled receptors self-assemble in dynamics simulations of model bilayers. *J Am Chem Soc* 129(33):10126–10132.
36. Jastrzebska B, et al. (2015) Disruption of rhodopsin dimerization with synthetic peptides targeting an interaction interface. *J Biol Chem* 290(42):25728–25744.
37. Jastrzebska B, et al. (2004) Functional characterization of rhodopsin monomers and dimers in detergents. *J Biol Chem* 279(52):54663–54675.
38. Gunkel M, et al. (2015) Higher-order architecture of rhodopsin in intact photoreceptors and its implication for phototransduction kinetics. *Structure* 23(4):628–638.
39. Applebury ML, et al. (2000) The murine cone photoreceptor: A single cone type expresses both S and M opsins with retinal spatial patterning. *Neuron* 27(3):513–523.
40. Munro S, Pelham HR (1987) A C-terminal signal prevents secretion of luminal ER proteins. *Cell* 48(5):899–907.
41. Park JH, Scheerer P, Hofmann KP, Choe HW, Ernst OP (2008) Crystal structure of the ligand-free G-protein-coupled receptor opsin. *Nature* 454(7201):183–187.
42. Kefalov VJ, et al. (2005) Breaking the covalent bond–a pigment property that contributes to desensitization in cones. *Neuron* 46(6):879–890.
43. Anderson JR, et al. (2009) A computational framework for ultrastructural mapping of neural circuitry. *PLoS Biol* 7(3):e1000074.
44. Molday LL, Cook NJ, Kaupp UB, Molday RS (1990) The cGMP-gated cation channel of bovine rod photoreceptor cells is associated with a 240-kDa protein exhibiting immunochemical cross-reactivity with spectrin. *J Biol Chem* 265(30):18690–18695.
45. Cornwall MC, Jones GJ, Kefalov VJ, Fain GL, Matthews HR (2000) Electrophysiological methods for measurement of activation of phototransduction by bleached visual pigment in salamander photoreceptors. *Methods Enzymol* 316:224–252.
46. Yokoyama R, Yokoyama S (2000) Comparative molecular biology of visual pigements. *Molecular Mechanisms in Visual Transduction*, eds Stavenga DG, de Grip W, Pugh E (Elsevier, New York), pp 257–296.
47. Nikonov SS, Kholodenko R, Lem J, Pugh EN, Jr (2006) Physiological features of the S- and M-cone photoreceptors of wild-type mice from single-cell recordings. *J Gen Physiol* 127(4):359–374.
48. Parry JW, Bowmaker JK (2000) Visual pigment reconstitution in intact goldfish retina using synthetic retinaldehyde isomers. *Vision Res* 40(17):2241–2247.
49. Govardovskii VI, Fyhrquist N, Reuter T, Kuzmin DG, Donner K (2000) In search of the visual pigment template. *Vis Neurosci* 17(4):509–528.
50. Makino CL, Groesbeek M, Lugtenburg J, Baylor DA (1999) Spectral tuning in salamander visual pigments studied with dihydroretinal chromophores. *Biophys J* 77(2):1024–1035.
51. Hubbard R, Kropf A (1958) The action of light on rhodopsin. *Proc Natl Acad Sci USA* 44(2):130–139.
52. Luo DG, Yau KW (2005) Rod sensitivity of neonatal mouse and rat. *J Gen Physiol* 126(3):263–269.